

## **TECHNICAL MEMORANDUM**

**Center for Multidisciplinary Research in Transportation  
Texas Tech University  
Lubbock, Texas 79409  
806-742-3037 – FAX 806-742-3488**

<b>Date:</b> 06/12/2023	<b>Study No:</b> 601CT0000029807
<b>To:</b> Larry Blackburn, P.E. ASM Rahman, Ph.D., P.E.	<b>Tech Memo No:</b> 601CT0000029807-TM1
<b>From:</b> Research Team	<b>Revision No:</b>
<b>Subject:</b> Evaluation of the Pavement Condition in Beltway 8 in Houston	

## **Table of Contents**

I.	Introduction .....	6
II.	Field Investigation .....	14
A.	Slab Deflection.....	14
B.	Soil Modulus from DCP and CPT .....	19
C.	Backfill/Subgrade Soil Characterization from Laboratory Tests.....	31
	Summary .....	35
	References .....	35

## List of Figures

Figure 1 Field Testing Location.....	6
Figure 2 Typical Pavement Section of CSJ: 0500-03-429.....	6
Figure 3 Distresses seen in the field .....	8
Figure 4 Tie Bar failure due to influence of Edge drainage (Fowler et al., 2012).....	9
Figure 5 Failed joint has separated and faulted (Fowler W et al., 2012).....	9
Figure 6 Test layout with the coring location where DCP and CPT test was carried out. Green dots represents where both DCP and CPT was performed, blue dot represents location where only DCP was performed, and red dot represents where DCP was performed but failed. ....	10
Figure 7 FWD testing at the test section.....	11
Figure 8 Coring Operation.....	11
Figure 9 Characterizing extracted Core Sample .....	12
Figure 10 DCP Testing .....	12
Figure 11 CPT Testing.....	13
Figure 12 Lidar operation .....	13
Figure 13 FWD testing location conducted on Day 1 and Day 2 .....	14
Figure 14 Colored profile map of variation of deflection measured from FWD test .....	14
Figure 15 FWD Testing Location and Deflection measured for Inside Shoulder .....	15
Figure 16 FWD Testing Location and Deflection measured for Inside Lane.....	15
Figure 17 FWD Testing Location and Deflection measured for Mid Lane .....	16
Figure 18 FWD Testing Location and Deflection measured for Outside Lane (Inside) .....	16
Figure 19 FWD Testing Location and Deflection measured for Outside Lane (Outside).....	17
Figure 20 Comparison between Outside Lane_in and Outside Lane_Out FWD testing Deflections .....	17
Figure 21 FWD Testing Location and Deflection measured for Outside Shoulder .....	18
Figure 22 FWD Deflections on all tested segments.....	18
Figure 23 Locations of DCP and CPT (OS = outside shoulder, OL = outside lane, ML = middle lane, IL = inside lane, IS = inside shoulder; RWP = right wheel path, and LWP = left wheel path) .....	19
Figure 24 Cumulative number of blow counts vs. penetration depth from DCP tests along the outside lane, left wheel path (OL LWP) from east to west.....	20
Figure 25 Cumulative number of blow counts vs. penetration depth from DCP tests conducted along outside lane to inside lane at (a) Location 2 and (b) Location 3.....	20
Figure 26 Subgrade moduli (a) along the outside lane, left wheel path from east to west, (b) at Location 2 from outside lane to inside lane, and (c) at Location 3 from outside lane to inside lane .....	22
Figure 27 Proximity of DCP and CPT location .....	24
Figure 28 CPT log from CPT3.....	24
Figure 29 CPT log from CPT5.....	25
Figure 30 CPT log from CPT6.....	26
Figure 31 CPT log from CPT7.....	27
Figure 32 CPT log from CPT8.....	28

Figure 33 Cone resistance vs. penetration depth from all five CPTs.....	29
Figure 34 Correlation between soil moduli from DCP and average cone resistances from CPT for the corresponding layers.....	29
Figure 35 Moduli of backfill materials and founding soils determined from CPT.....	30
Figure 36 Photos showing (a) soils retained on each sieve during wet sieving for CPT2 sample from 20" to 27", (b) CPT2 sample from 27" to 32.5 ", (c) CPT5 sample from 20" to 30", and (d) hydrometer testing in progress.....	33
Figure 37 Particle size distributions curves of all soil samples .....	34

## **List of Tables**

Table 1 Summary of DCP and CPT performed in the project location .....	10
Table 2 Weighted average value of subgrade modulus at each DCP location. ....	23
Table 3 Summary of laboratory test results .....	34

## I. Introduction

A request was made under the inter-agency contract (IAC Contract No. 601CT0000029807) by the Houston District to conduct field testing, gather and analyze data to identify the causes of distresses on Beltway 8 Westbound Mainlane, Harris County (Figure 1). The IH45/Beltway 8 (South) Interchange (CSJ: 0500-03-429) has been in operation since 1997, and the pavement structure consists of 12" CRCP + 1" ASB + 6" PCTB + 6" LTS. The structure was placed above cement stabilized Backfill with a support from mechanically stabilized embankment (MSE) on westbound and 4:1 slope maintained slope Embankment on eastbound (Figure 2).

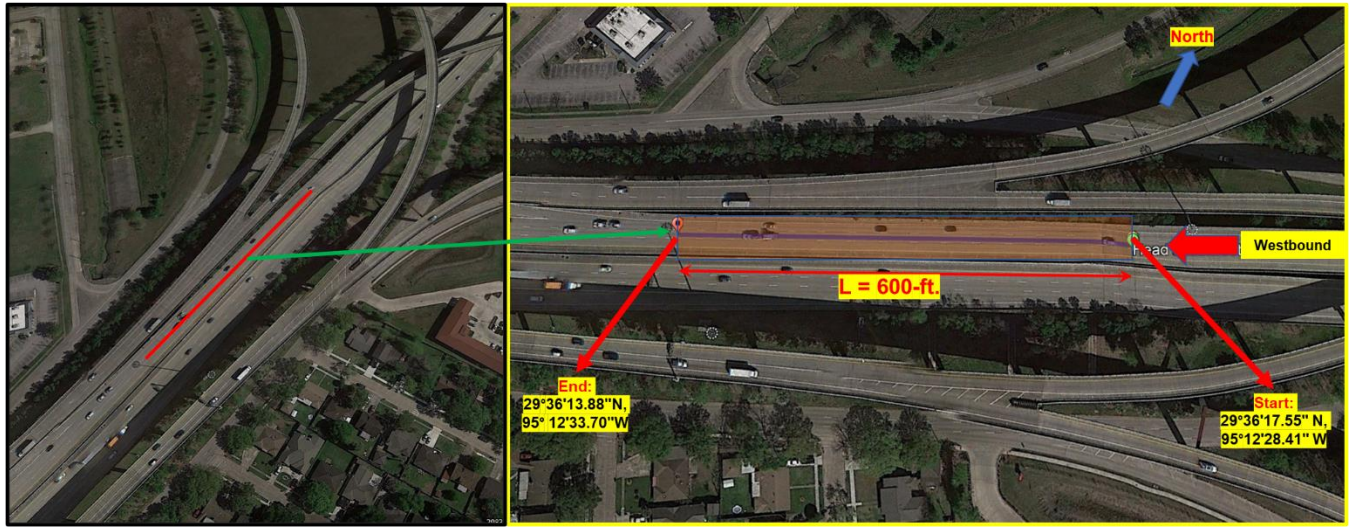


**Figure 1** Field Testing Location

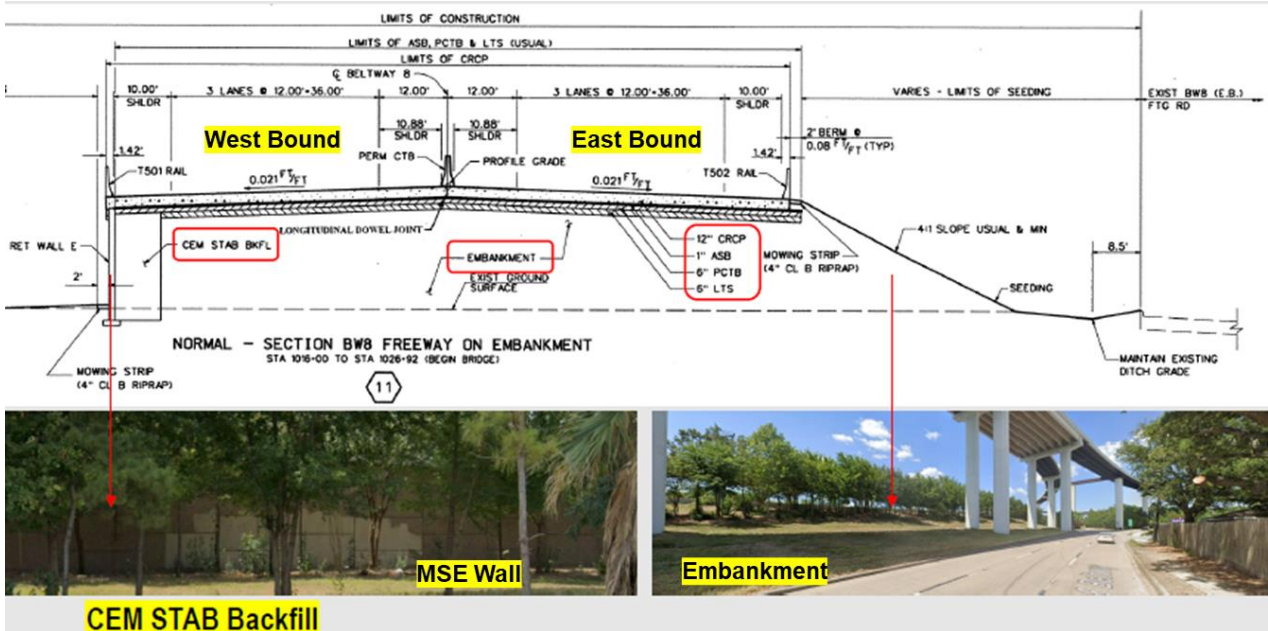


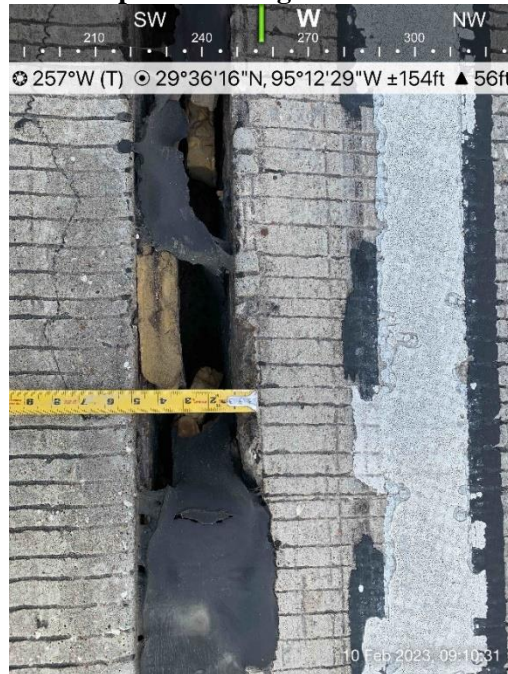
**Figure 2** Typical Pavement Section of CSJ: 0500-03-429

The condition of the subject section was evaluated onsite and lane separation, faulting, and settlement were the major distresses observed. These distresses lead to uneven roadway surfaces, which have the potential to result in serious accidents at highway speeds. Also, the depressed slab which is below the design grade collects water that could cause hydroplaning or ice formation during freezing temperatures. **Figure 3** presents some of the sections with lane separation, faulting, settlement and tilting of retaining wall observed in the site.

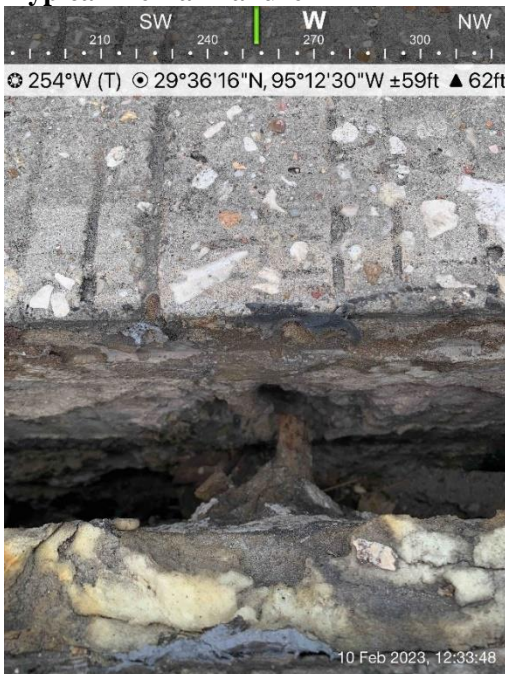
**3.a. Typical Lane Separation**



**3.b. Lane Separation ranges from 2 – 5 inches**



**3.c. Typical Tie Bar Failure**



**3.d. Faulting**



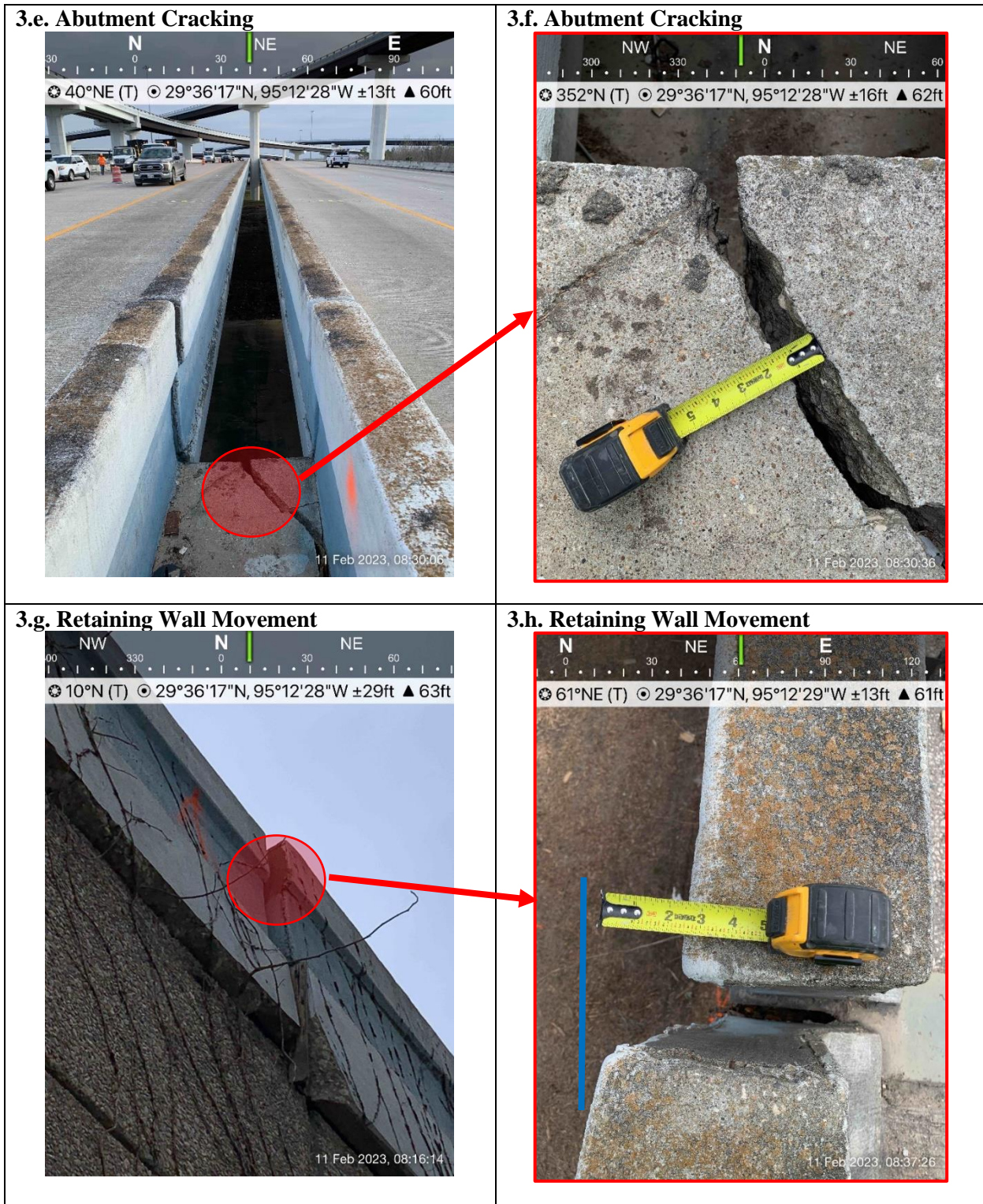


### **Figure 3 Distresses seen in the field**

According to Fowler et al. (2012), there is a limited understanding of the mechanisms underlying lane separation and faulting occurrences in pavement. Environmental factors such as temperature and moisture can cause distortion and warping in the slab, particularly in regions with poor drainage and expansive soils. The movement of the pavement structure can subsequently cause the outer shoulder slab to shift up

or down, creating a lever arm that is restrained by tie bars, as illustrated in [Figure 4](#). Cyclic variations in temperature and moisture facilitate the ingress of water and non-compressible debris into the joint, significantly increasing the stress on the tie bar. Additionally, the presence of free moisture within the joint leads to gradual corrosion of the tie bar until reduced section ruptures or pull-out failure occurs. As multiple tie bars in a row fail, the slabs become disengaged, allowing more water to infiltrate the joint, ultimately resulting in sub-base support deterioration.

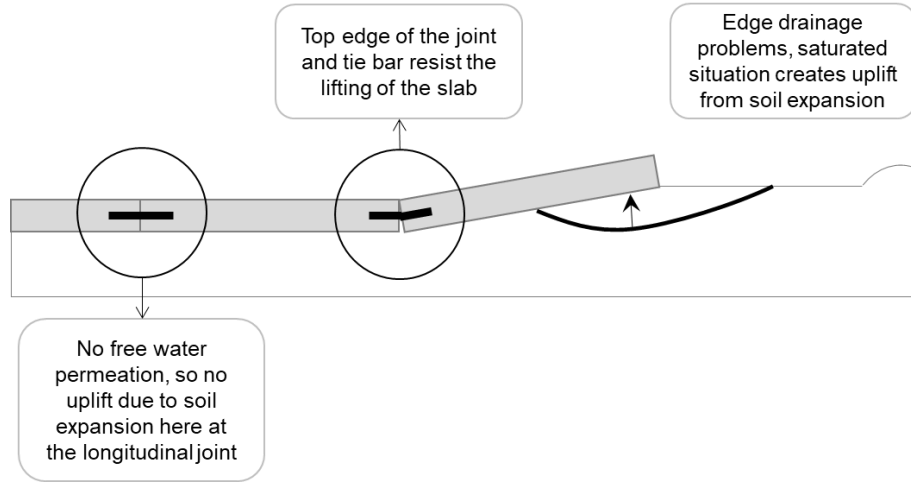


**Figure 4** Tie Bar failure due to influence of Edge drainage (Fowler et al., 2012)

As vertical friction is lost at the longitudinal joint, wheel load transfer across the joint becomes compromised, leading to the failure of the slab. When traffic traverses the longitudinal joint, the adjacent slabs move independently, with the slab carrying the majority of the wheel load deflecting more than the other. This deflection creates a pumping action during wet weather, allowing water to infiltrate the failed joint and removing waterborne fines from the sub-base. This cycle of sub-base softening and removal creates a substantial void beneath the slabs, which ultimately results in permanent subsidence or faulting, as illustrated in [Figure 5](#).

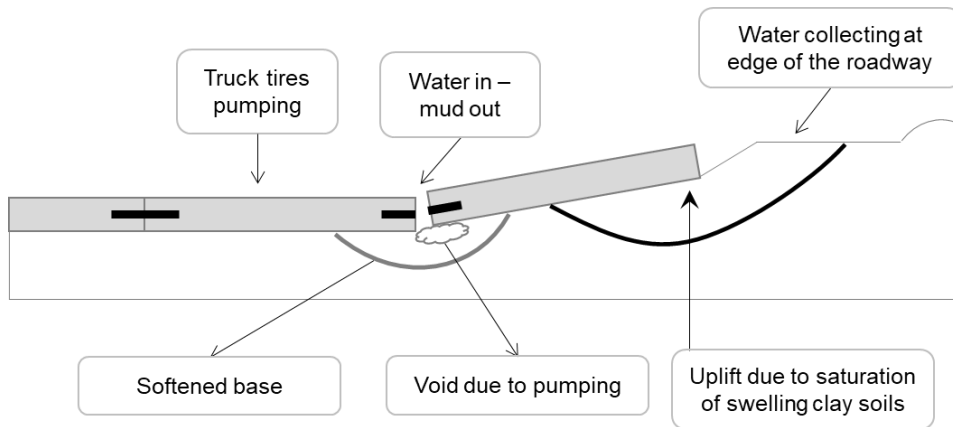


**Figure 5** Failed joint has separated and faulted (Fowler et al., 2012).

[Figure 6](#) illustrates the project location as well as the locations where 17 cores were taken. To identify the causes of the pavement distresses observed in the subject project, field testing was conducted on February 10, 2023, and February 11, 2023. The field testing conducted covered deflection testing with FWD from 29°36'17.55" N, 95°12'28.41" W up to 29°36'13.88" N, 95° 12'33.70" W traversing about 600-feet in

length. In addition, coring, dynamic cone penetrometer (DCP) testing, Cone Penetration Test (CPT), Ground Penetration Radar (GPR), Lidar, and MIRA testing were also conducted. Soil samples were obtained from cored locations and various soil testing activities, including the Atterberg limits, hydrometer test, moisture content and wet sieve analysis were performed.

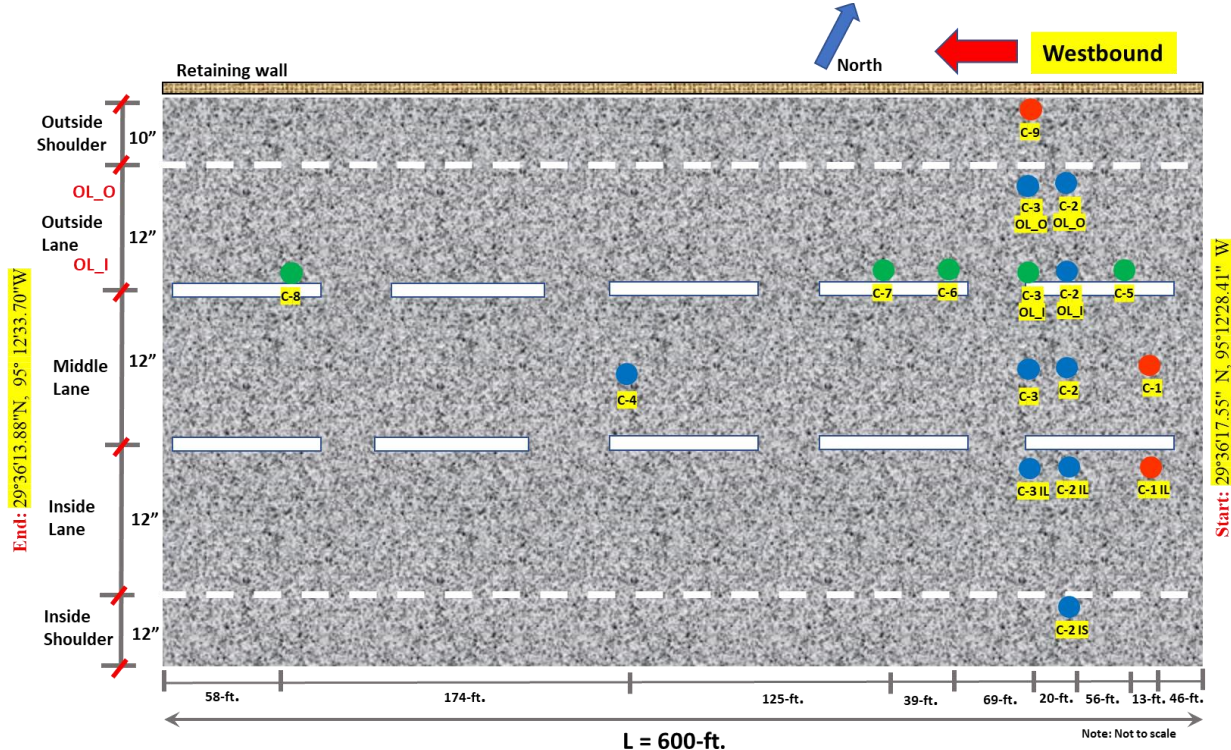


**Figure 6** Test layout with the coring location where DCP and CPT test was carried out. Green dots represent where both DCP and CPT was performed, blue dot represents location where only DCP was performed, and red dot represents where DCP was performed but failed.

**Table 1** tabulates the DCP and CPT which were carried out in 17 core locations. Five locations were tested using both CPT and DCP. Out of 17 core locations, 3 locations where DCP was performed failed which is marked in red. Thus, the result from those three locations for DCP is not included in this report. Also, the GPR and Lidar were performed in the project location by TxDOT representative. The result for same is not included in this report.

**Table 1** Summary of DCP and CPT performed in the project location.

Lane	C1	C2	C3	C4	C5	C6	C7	C8	C9
Outside Shoulder(OS)									
Outside Lane - Outside (OL_O)		DCP	DCP						
Outside Lane - Inside (OL_I)		DCP	CPT + DCP						
Mid Lane (ML)	DCP	DCP	DCP	DCP	CPT + DCP	CPT + DCP	CPT + DCP	CPT + DCP	DCP
Inside Lane (IL)	DCP	DCP	DCP						
Inside Shoulder (IS)		DCP							

Figures 7 to 12 show the FWD, coring, characterization of extracted core sample, DCP testing, CPT testing and Lidar activities, respectively, which were conducted in the field. Based on all the information gathered, this report is prepared to aid TxDOT in its efforts to come up with appropriate rehabilitation strategies.



**Figure 7** FWD testing at the test section



**Figure 8** Coring Operation



**Figure 9** Characterizing extracted Core Sample



**Figure 10** DCP Testing



**Figure 11** CPT Testing



**Figure 12** Lidar operation

The following sections present the results of the testing conducted during the field and laboratory testing for the distresses of project site.

## II. Field Investigation

This section presents the results of the testing conducted.

### A. Slab Deflection

Deflections on the slab were evaluated on all the lanes. [Figure 13](#) shows FWD drop location as performed in the project site. FWD test was conducted on 10<sup>th</sup> and 11<sup>th</sup> February 2023, referred as Day 1 and Day 2 respectively. The first day (i.e., Day 1) FWD testing was conducted in Inside Shoulder, Inside Lane and Middle Lane. The second day (i.e., Day 2) FWD testing was conducted in Outside Lane (In), Outside Lane (Out) and Outside shoulder. The deflections at 9,000-lb loading were evaluated along all the lanes covering a total length of 600-ft each.

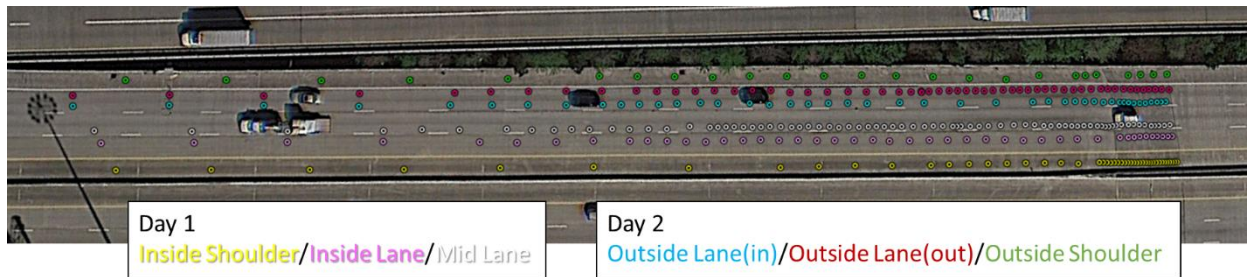


**Figure 13** FWD testing location conducted on Day 1 and Day 2

[Figure 14](#) shows the colored profile of variation of deflection measured during FWD test. Green color indicates a minimum deflection of 0 while the red color indicates the maximum deflection of 24 mils recorded in the subject project. From the figure, we can infer that the location around DMI 40-ft have recorded the highest deflection. In the subsequent sections, further discussion on the deflection results will be presented.

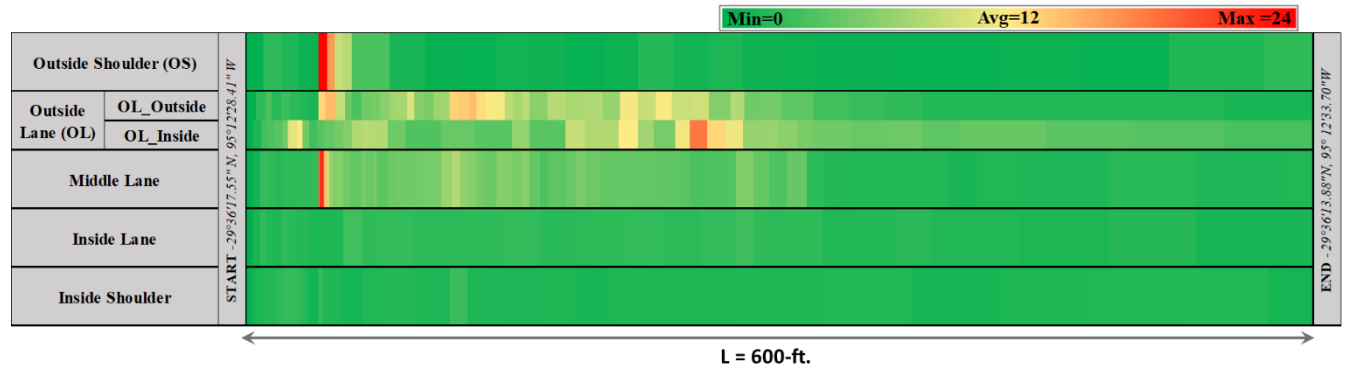


**Figure 14** Colored profile map of variation of deflection measured from FWD test

#### Inside Shoulder

It can be observed that the deflections were generally between 1 to 3.5 mils as illustrated in [Figure 15](#). This indicates the pavement condition and performance of the Inside shoulder is in pretty good shape.

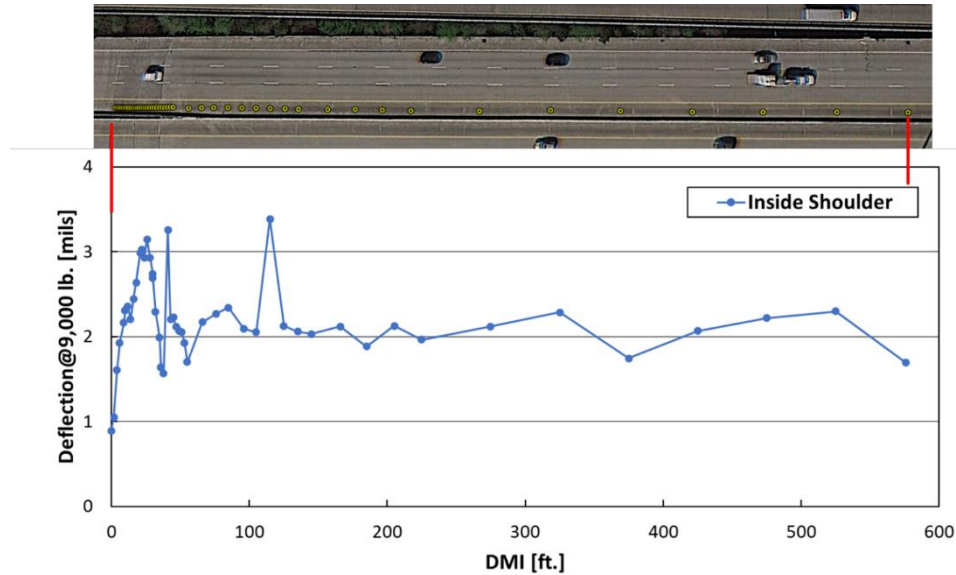


**Figure 15** FWD Testing Location and Deflection measured for Inside Shoulder Inside Lane

### Inside Lane

Similarly, as shown in [Figure 16](#), it can be observed that the deflections were generally lower than 4 mils indicating a sound pavement condition and the performance in this section is still acceptable.

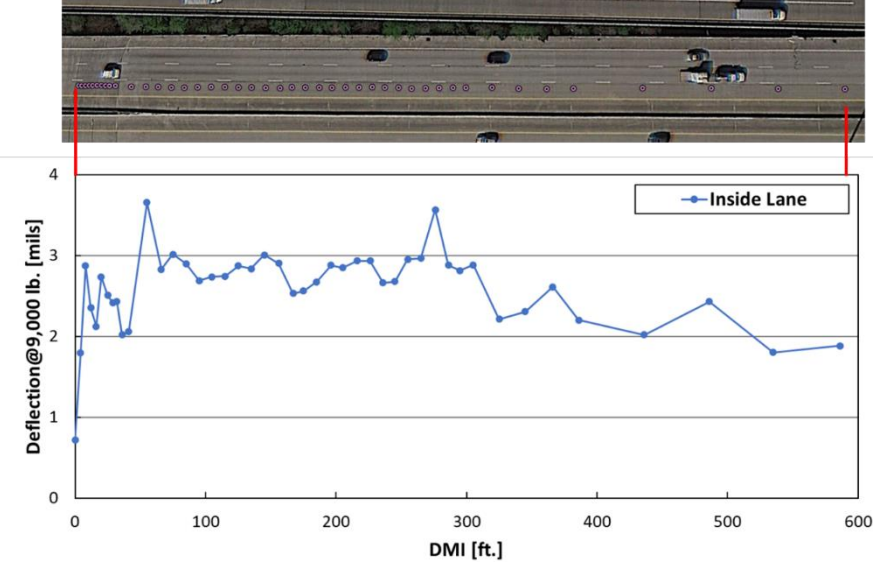


**Figure 16** FWD Testing Location and Deflection measured for Inside Lane

### Middle Lane

However, compared to the Inside shoulder and the Inside Lane, the Middle-Lane performance in FWD testing shows a poor condition as illustrated in [Figure 17](#). While the maximum deflection observed ranges from 0.4 to 24 mils, the majority of the deflections within the segment is between 4 to 9 mils which is greater than the statewide average deflections for a 12-in CRCP. This significant variability may signify

the existence of some critical issues in the sublayer of the pavement. Specifically, the DMI between 41-ft to 44-ft generated high deflection.

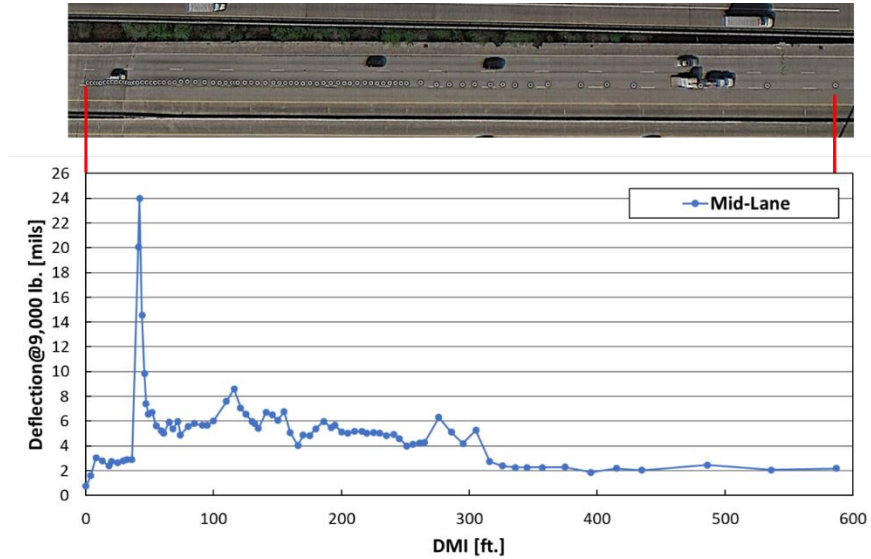


**Figure 17** FWD Testing Location and Deflection measured for Mid Lane

### Outside Lane

For the Outside Lane, FWD test was conducted twice. The first one was at the Outside lane covering Inside zone (OL\_I) and the second one was at the Outside lane covering Outside Zone (OL\_O). The result for both is presented below. Comparing both the FWD test, it is observed that OL\_I recorded the maximum deflection of 19.28 mils, whereas the OL\_O recorded the maximum deflection of 15 mils as seen in [Figure 18](#) and [Figure 19](#) respectively.

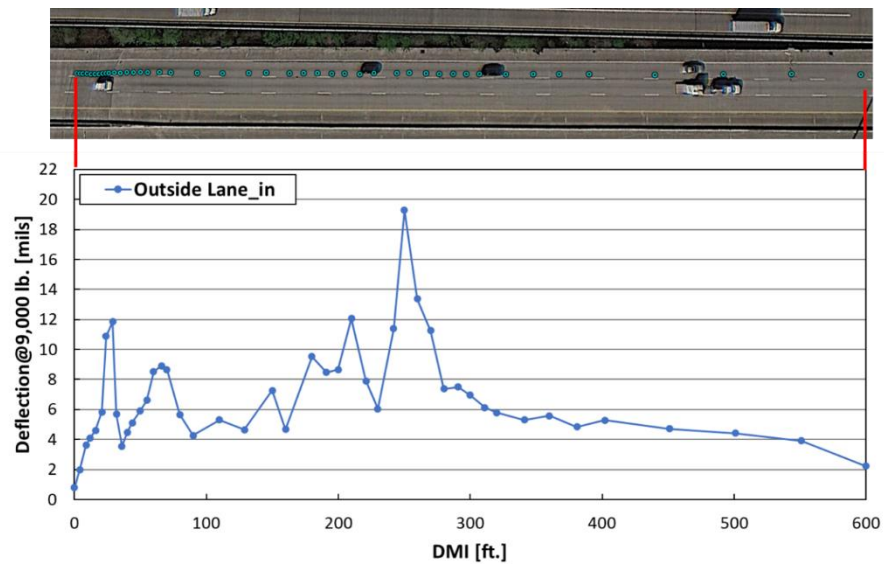


**Figure 18** FWD Testing Location and Deflection measured for Outside Lane (Inside)

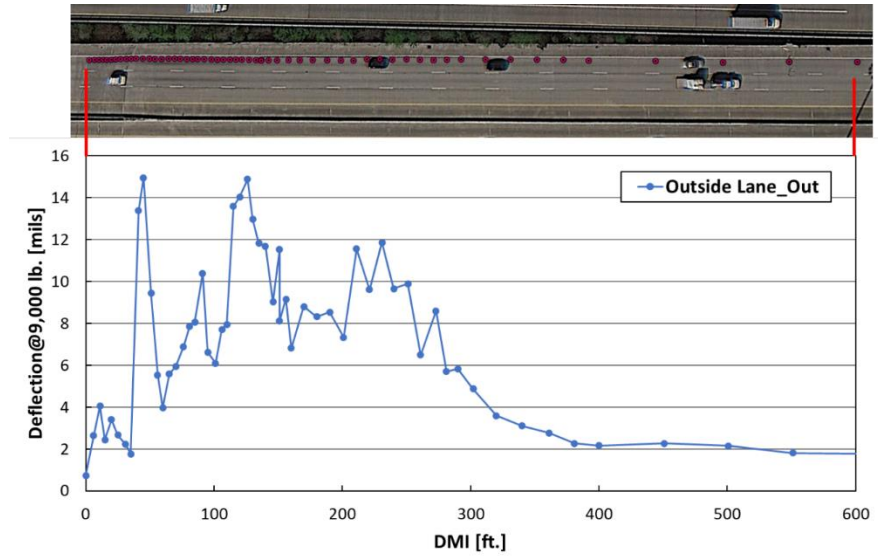


**Figure 19** FWD Testing Location and Deflection measured for Outside Lane (Outside)

**Figure 20** shows the comparison between Outside Lane\_in and Outside Lane\_out FWD testing deflection. In both the test segments, DMI between 40-ft to 300-ft recorded a higher value of deflection indicating presence of severe distresses.

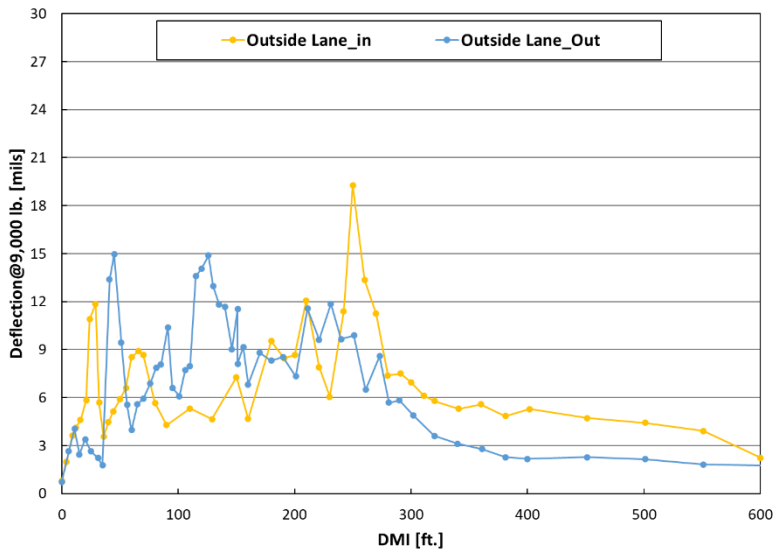


**Figure 20** Comparison between Outside Lane\_in and Outside Lane\_Out FWD testing Deflections

#### Outside Shoulder

The maximum FWD measured deflection observed in case of Outside Shoulder is 26.83 mils at DMI 41 as shown in **Figure 21**. The DMI is between 41-ft to 60-ft.

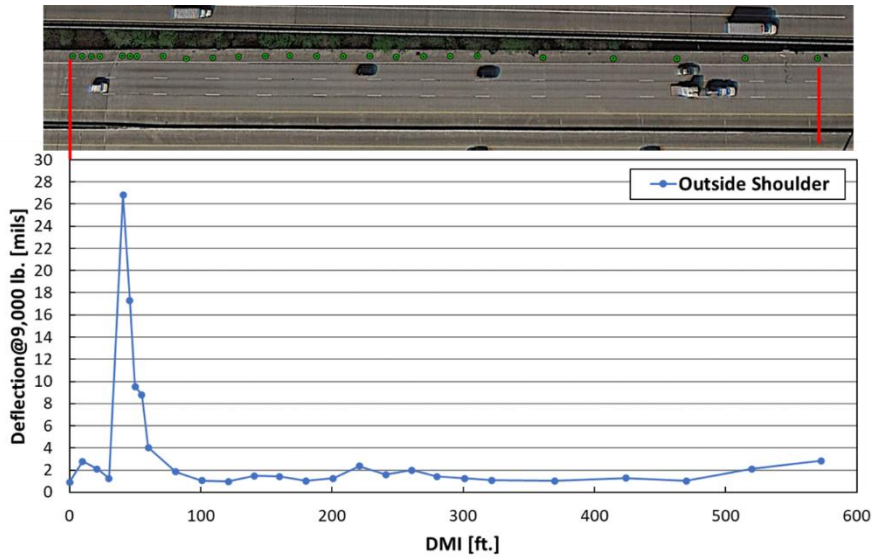


**Figure 21** FWD Testing Location and Deflection measured for Outside Shoulder

In Summary, [Figures 22](#) summarize the FWD deflections of all the segments tested in all lanes. It can be observed that the high deflections occur between DMI 0 to 300-ft.

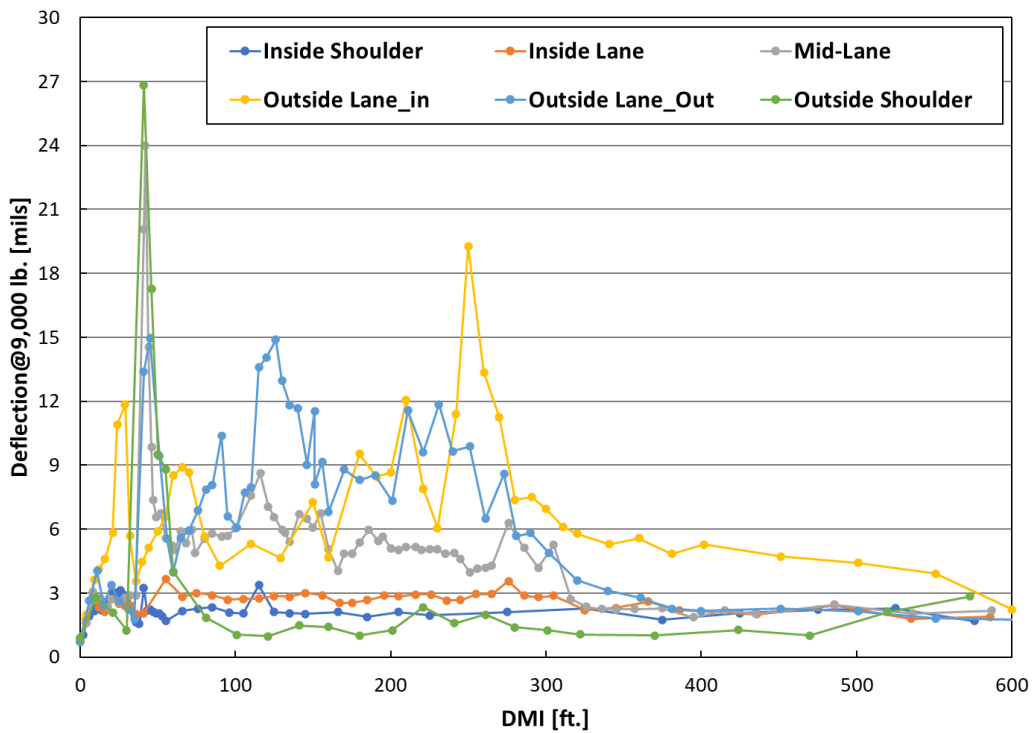


**Figure 22** FWD Deflections on all tested segments

## B. Soil Modulus from DCP and CPT

To estimate backfill/subgrade conditions in the embankment area, dynamic cone penetration (DCP) tests were conducted at 17 locations. Locations and names of DCP tests conducted at the project site are shown in [Figure 23](#). Naming conventions are as follows: OS = outside shoulder, OL = outside lane, ML = middle lane, IL = inside lane, IS = inside shoulder, RWP = right wheel path, and LWP = left wheel path. Two tests (DCP4 and DCP8) out of 17 test locations were performed as control sections at locations where relatively less distresses were observed. Additionally, cone penetration tests (CPT) were conducted at five locations, also shown in Figure.

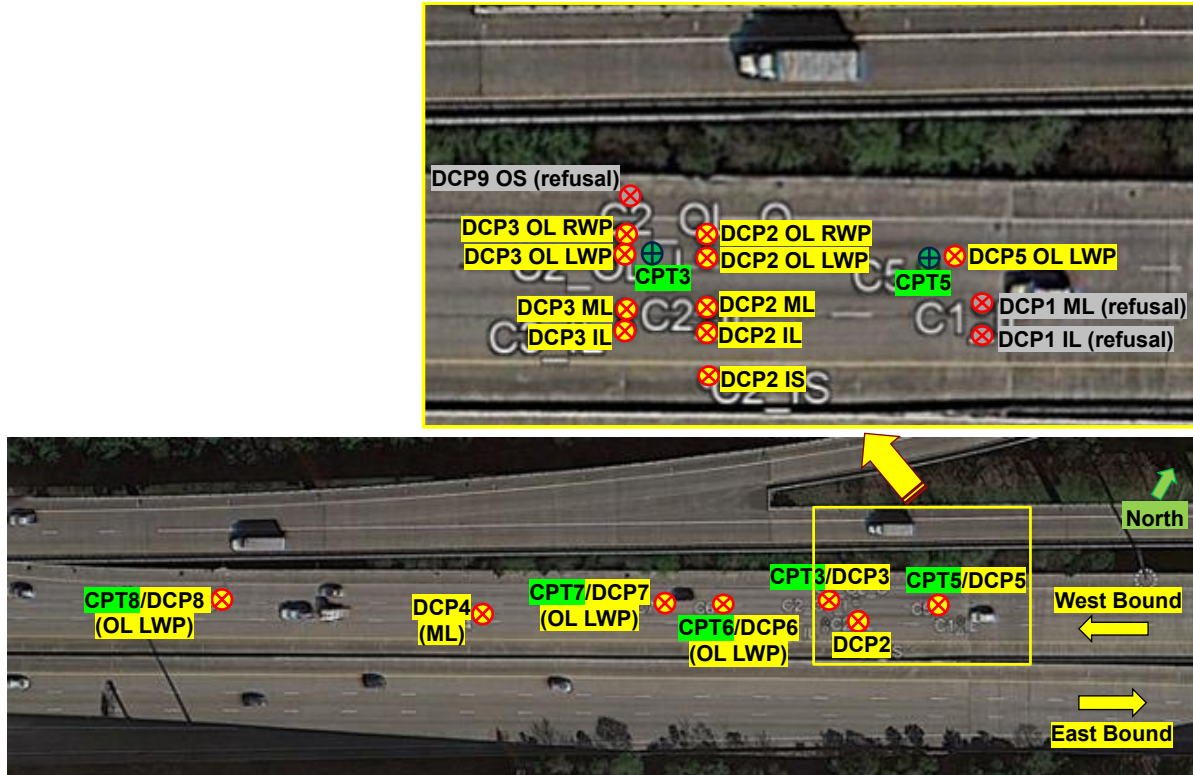


**Figure 23** Locations of DCP and CPT (OS = outside shoulder, OL = outside lane, ML = middle lane, IL = inside lane, IS = inside shoulder; RWP = right wheel path, and LWP = left wheel path)

DCP tests were conducted through the cored or drilled holes, and investigation depth varied from 81.4 in (6.8 ft) to 102.7 in (8.6 ft) below the pavement surface. Out of 17 DCP tests, three tests (DCP1 ML, DCP1 IL, and DCP9 OS) had refusals, indicating presences of the cement-treated backfills. [Figure 24](#) shows the cumulative blow counts vs. depth from DCP tests conducted along the outside lane, left wheel path (OL LWP) from east to west of the test section. The slope of the cumulative DCP blow counts vs. depth curve represents the penetration rate (*i.e.*, penetration depth per blow), and the steeper slope indicates a larger penetration rate or lower modulus of soil. [Figure 24](#) clearly indicates that backfill/subgrade conditions at the test locations were generally weaker than those at the control sections.

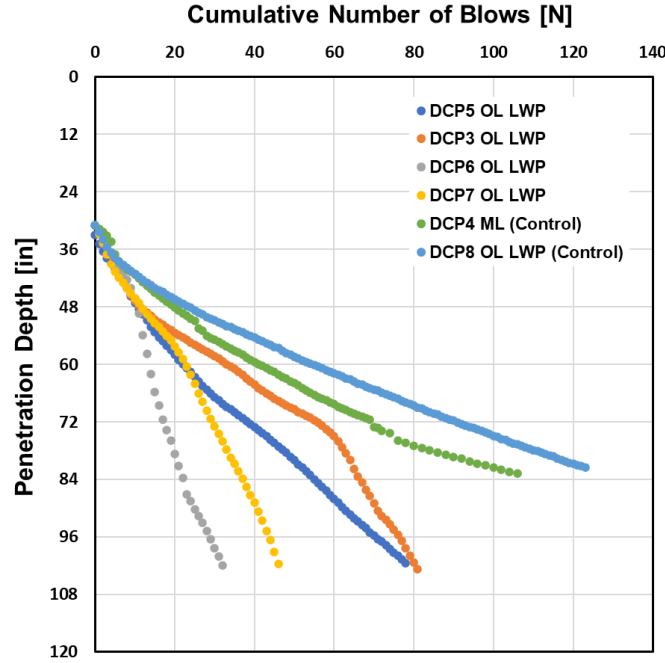


**Figure 24** Cumulative number of blow counts vs. penetration depth from DCP tests along the outside lane, left wheel path (OL LWP) from east to west

Figure 25 shows the cumulative blow counts vs. depth from DCP tests conducted along the outside lane to inside lane at Location 2 (Figure 25(a)) and Location 3 (Figure 25(b)). In general, the subgrade conditions at middle and inside lanes were weaker than those at outside lane for both Locations 2 and 3.

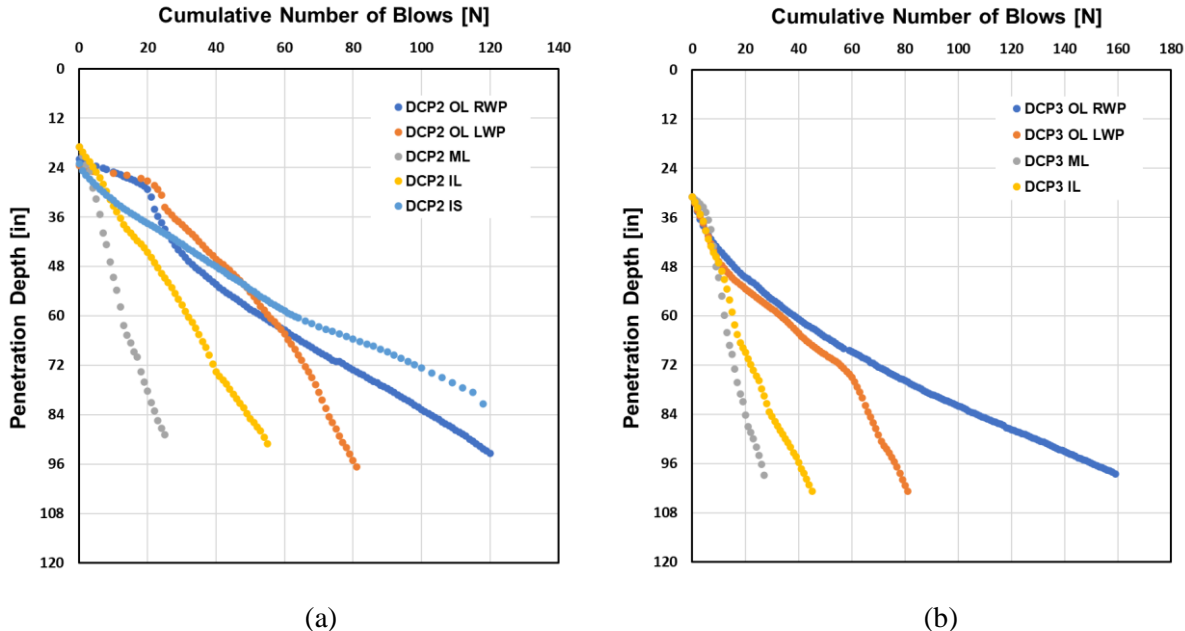
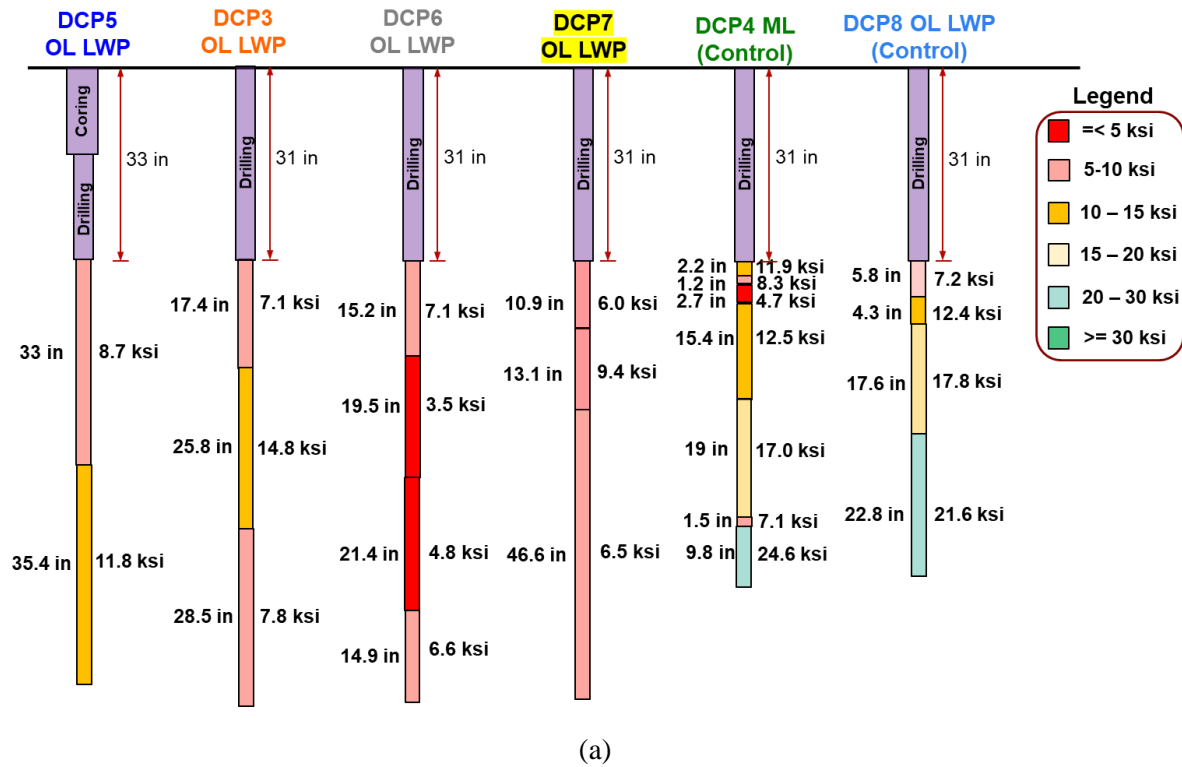


**Figure 25** Cumulative number of blow counts vs. penetration depth from DCP tests conducted along outside lane to inside lane at (a) Location 2 and (b) Location 3.

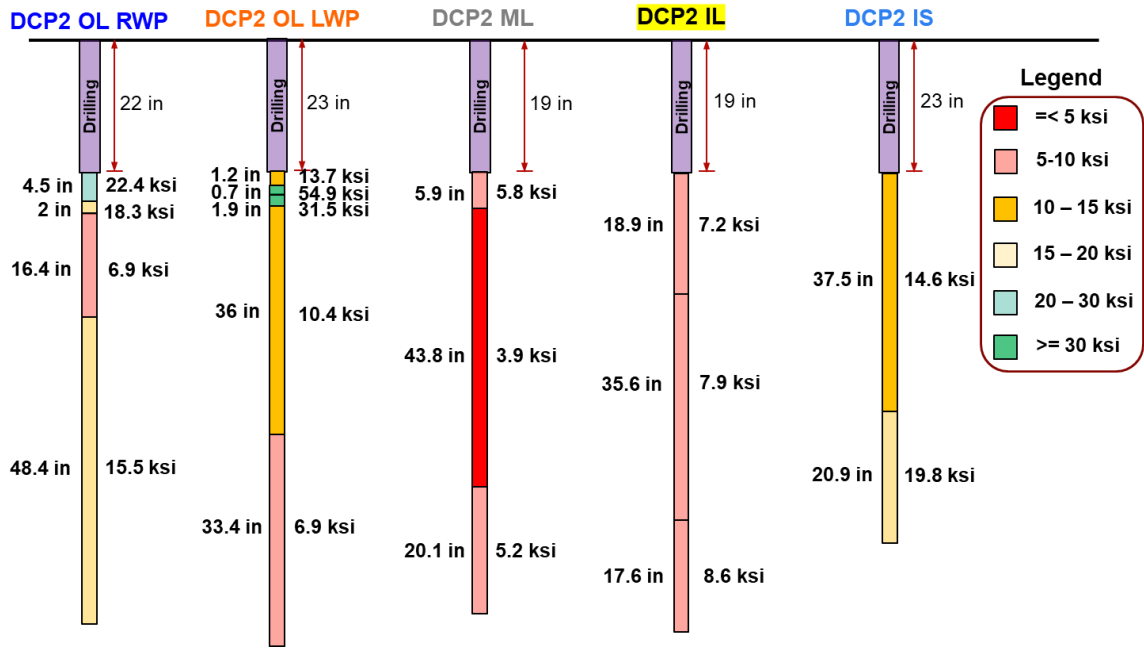
Using the penetration rates determined from cumulative blow counts vs. depth curves, subgrade moduli ( $M_r$ ) were estimated using the following equation:

$$M_r[\text{ksi}] = 2.55 CBR^{0.64} \text{ where } CBR = \frac{292}{PR^{1.12}} \text{ (PR = penetration rate in mm/blow)} \quad \text{Eq. (1)}$$

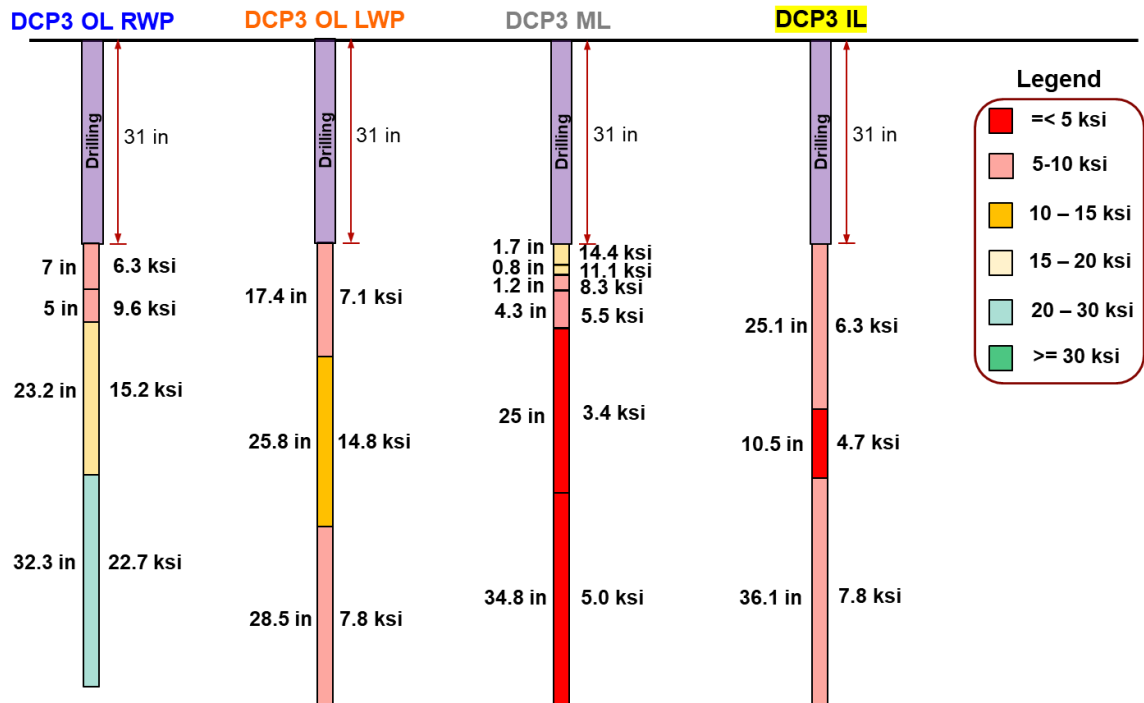
Figure 26 shows subgrade moduli obtained from Eq. (1) for all 15 non-refusal DCP tests.



(a)



(b)



(c)

**Figure 26** Subgrade moduli (a) along the outside lane, left wheel path from east to west, (b) at Location 2 from outside lane to inside lane, and (c) at Location 3 from outside lane to inside lane

Using the thicknesses and moduli of subgrade soils shown in [Figure 26](#), weighted average values of backfill/subgrade moduli were computed at each location and are presented in Table 1. At control sections, weighted average values of moduli were 15.8 ksi at DCP4 ML and 17.8 ksi at DCP8 OL LWP. On the other hand, results from DCP2 OL LWP, DCP2 ML, DCP2 IL, DCP3 ML, DCP3 IL, DCP6 OL LWP, and DCP7 OL LWP tests show that the weighted subgrade moduli at these locations are less than 10 ksi. These locations are highlighted in red in [Table 2](#).

**Table 2** Weighted average value of subgrade modulus at each DCP location.

Test Location	Investigation depth below pavement surface (in)	Weighted subgrade modulus (ksi)
<b>Along the outside lane, left wheel path from east to west</b>		
DCP5 OL LWP	101.4	10.3
DCP3 OL LWP	102.7	10.2
<b>DCP6 OL LWP</b>	<b>102.0</b>	<b>5.3</b>
<b>DCP7 OL LWP</b>	<b>101.6</b>	<b>7.0</b>
DCP4 ML (Control)	82.8	15.8
DCP8 OL LWP (Control)	81.5	17.8
<b>At Location 2 from outside lane to inside lane</b>		
DCP2 OL RWP	93.3	14.0
<b>DCP2 OL LWP</b>	<b>96.7</b>	<b>9.8</b>
<b>DCP2 ML</b>	<b>88.8</b>	<b>4.4</b>
<b>DCP2 IL</b>	<b>91.1</b>	<b>7.9</b>
DCP2 IS	81.4	16.4
<b>At Location 3 from outside lane to inside lane</b>		
DCP3 OL RWP	98.5	17.4
DCP3 OL LWP	102.7	10.2
<b>DCP3 ML</b>	<b>98.8</b>	<b>4.8</b>
<b>DCP3 IL</b>	<b>102.7</b>	<b>6.8</b>

As shown in [Table 2](#), the maximum DCP investigation depth was 102.7 in (= 8.6 ft) at Location 3, whereas the height of the embankment at Location 3 was about 17.8 ft (the maximum height of the embankment was about 25 ft in the vicinity of the bridge abutment). To investigate conditions of backfill/subgrade at deeper depths of the embankment, cone penetration tests were conducted by Terracon Consultants, Inc. As presented previously in [Figure 23](#), CPTs were performed at Locations 3, 5, 6, 7, and 8 in the proximity of the corresponding DCP tests, typically within 2 ft from the corresponding DCP locations (see [Figure 27](#)). [Figures 28 through 32](#) show the CPT logs provided by Terracon.

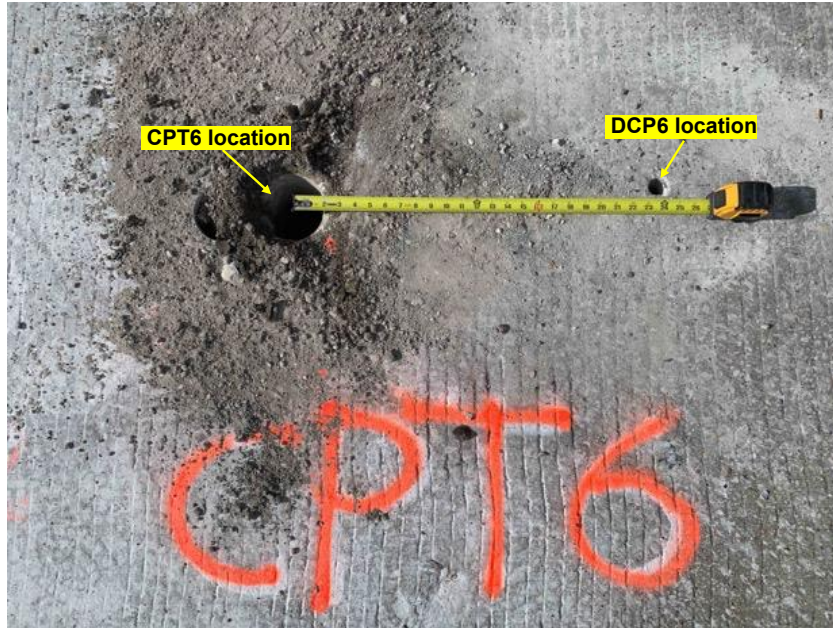


**Figure 27** Proximity of DCP and CPT location

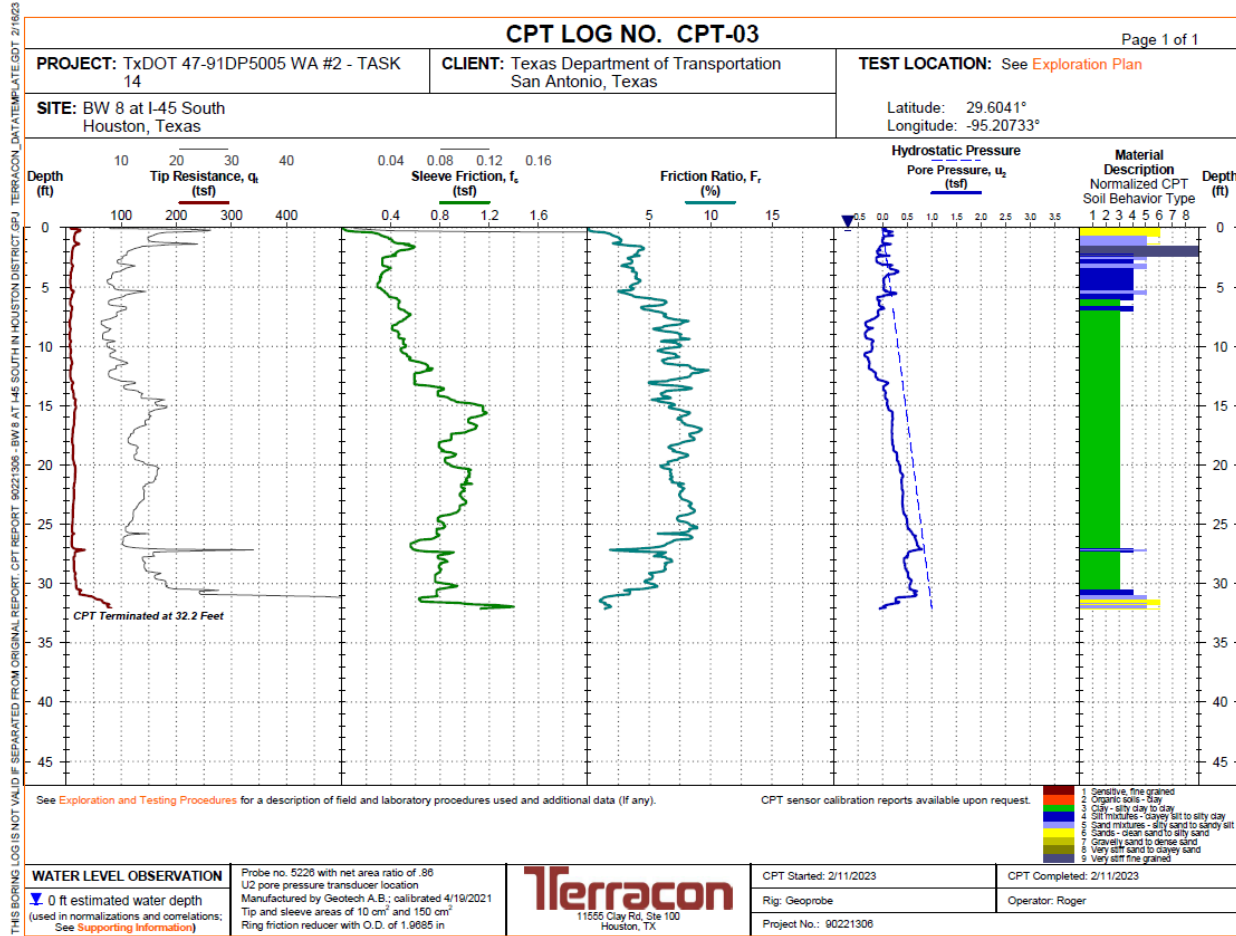


**Figure 28** CPT log from CPT3

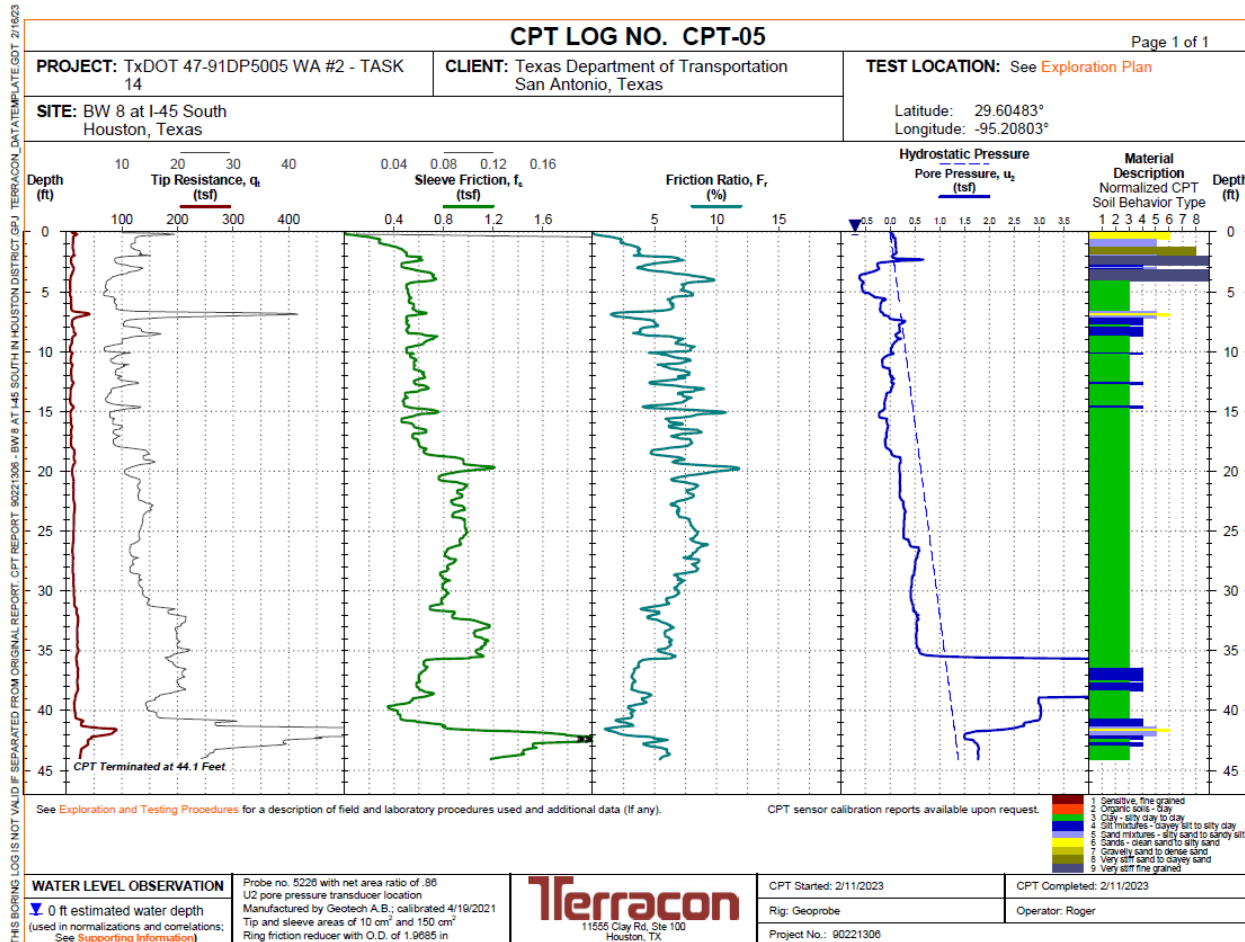


**Figure 29** CPT log from CPT5

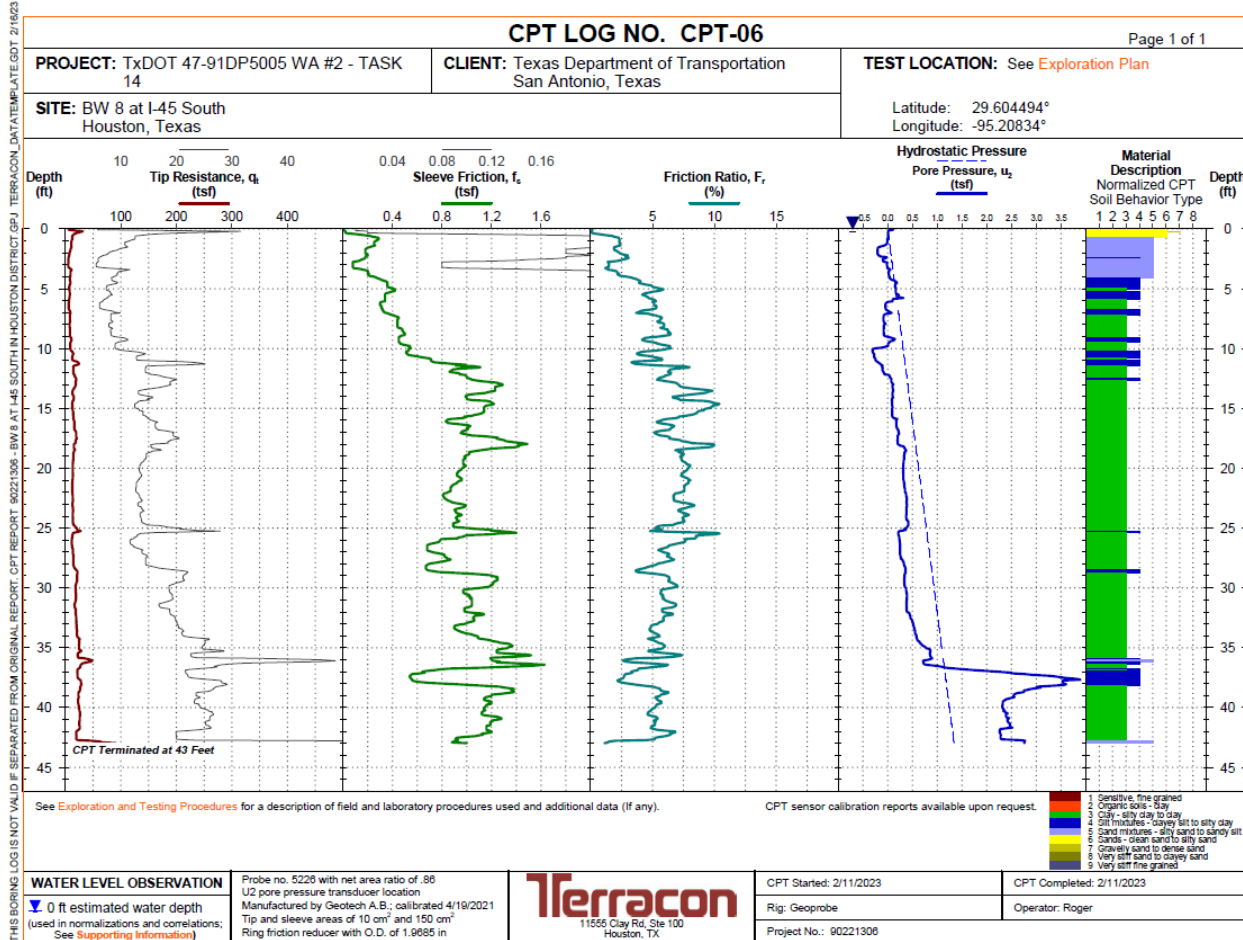


**Figure 30** CPT log from CPT6

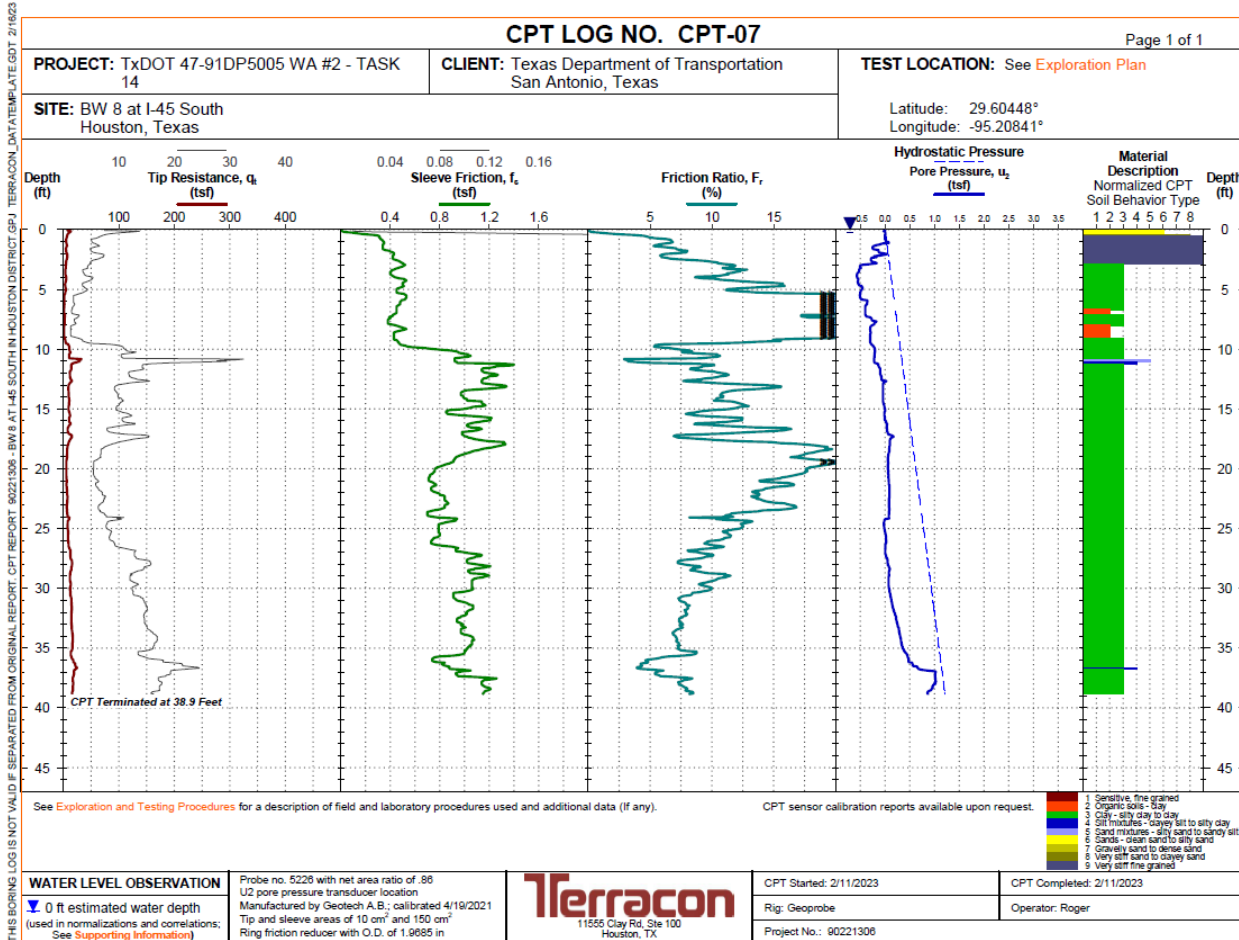


**Figure 31** CPT log from CPT7

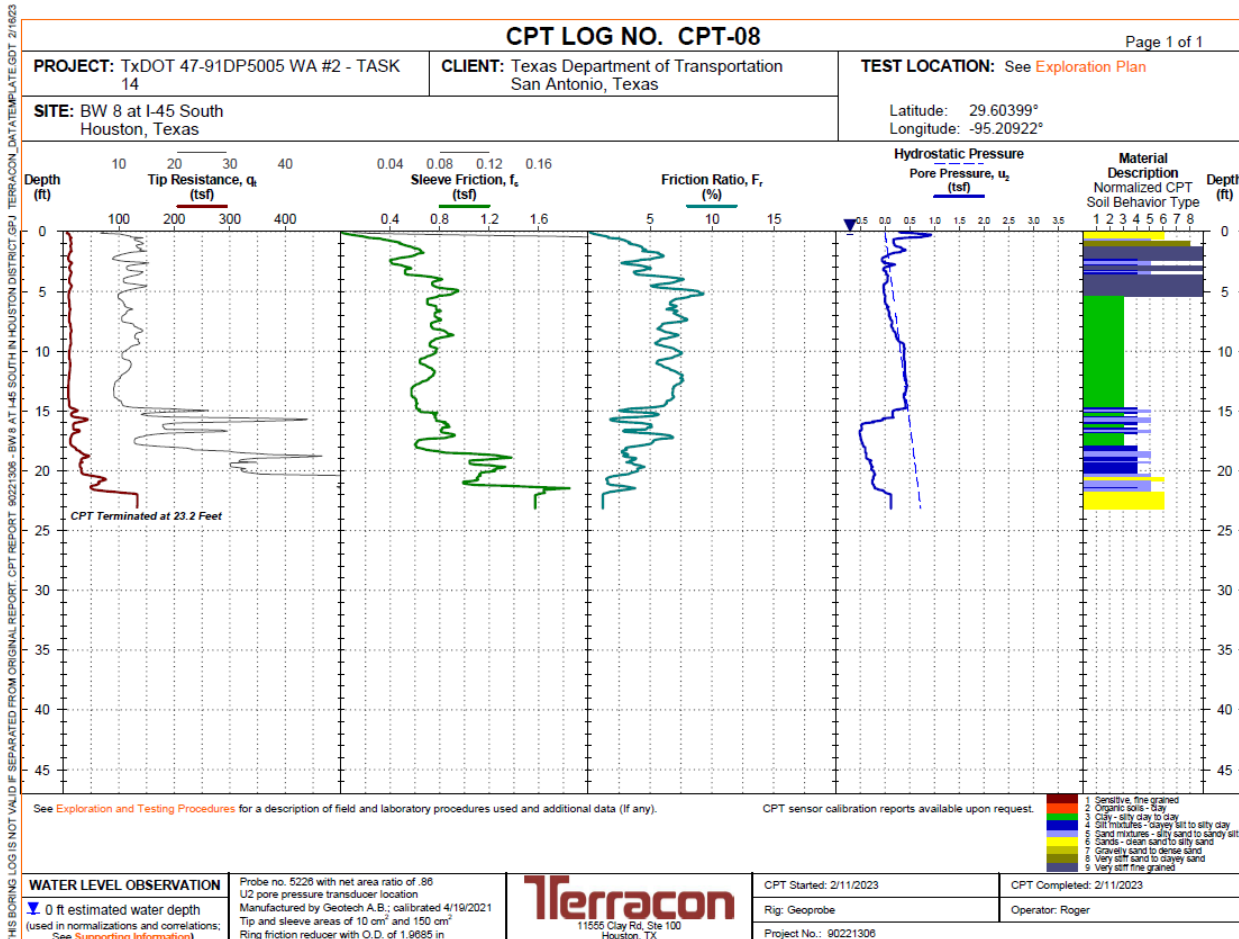


**Figure 32** CPT log from CPT8

Soil behavior type charts in all CPT logs suggest that the backfill materials in the embankment are predominantly clayey soils, except for sandy soils at very shallow depths. This is confirmed by detailed laboratory test results, presented later, from the soil samples collected at Location 2. For comparison purposes, cone resistances from all five CPTs are plotted in [Figure 33](#). It is observed that cone resistance values from a depth of about 2.5 ft to 20 ft below the pavement surface are typically less than 15 tsf. Also, overall, CPT8 (control section) shows the largest cone resistance values and CPT7 shows smallest values. Variations of cone resistance up to a depth of 9 ft (108 in), which was about maximum depth of DCP tests, are also presented in [Figure 33](#).

Results from CPTs are commonly used to estimate engineering properties of soils such as friction angle and relative density for sandy soils and undrained shear strength for clayey soils. Unfortunately, very limited research was done on the relationship between cone resistance and resilient modulus, and there are no well accepted correlations between them in the literature. Therefore, to empirically determine the soil moduli using the CPT results, a correlation study between soil moduli estimated from DCP results and cone resistances from CPTs was performed for the project site. At locations where both DCP and CPT tests were performed (*i.e.*, Locations 3, 5, 6, 7, and 8), the thicknesses and moduli of embankment backfill/subgrade layers were estimated from DCP (see [Figure 26](#)) and the soil modulus of each layer was

compared with the average cone resistance from CPT for the corresponding layer. Then, regression analysis was performed to establish correlation between soil modulus from DCP and cone resistance from CPT, as shown in [Figure 34](#). The soil moduli were then determined using the cone resistance and established correlation and are presented in [Figure 35](#).

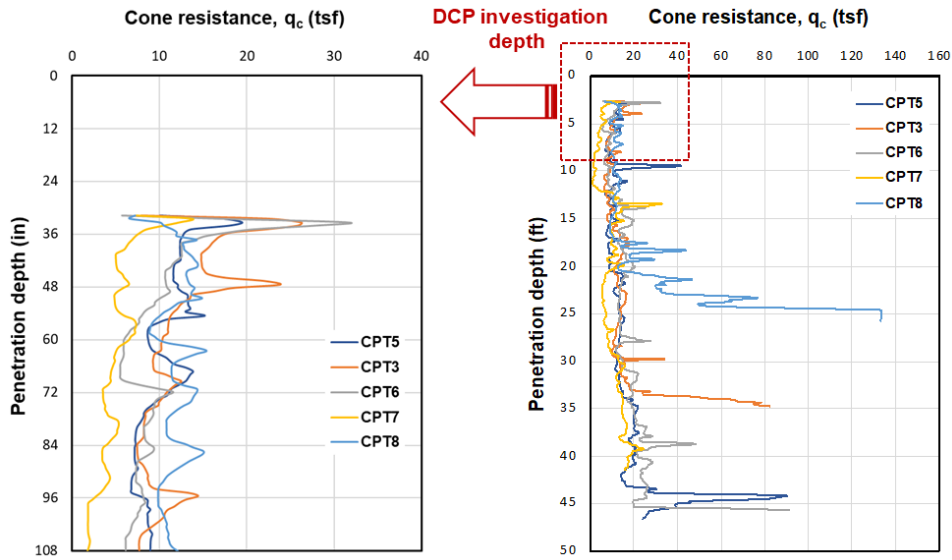


**Figure 33** Cone resistance vs. penetration depth from all five CPTs

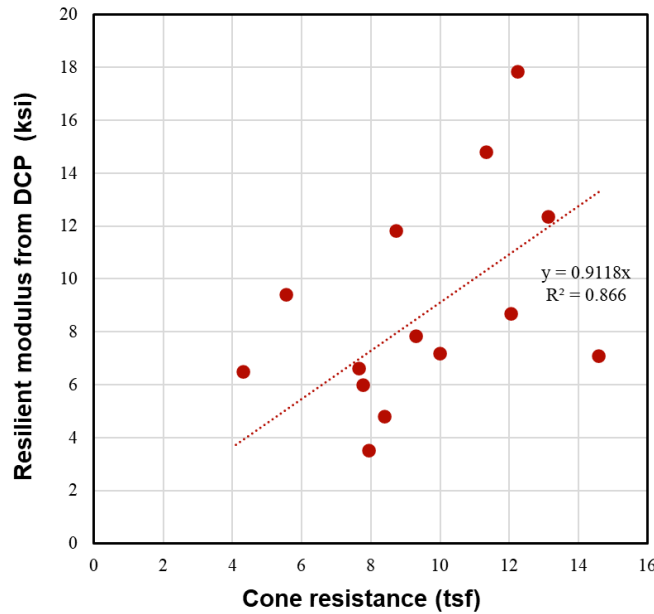


**Figure 34** Correlation between soil moduli from DCP and average cone resistances from CPT for the corresponding layers.

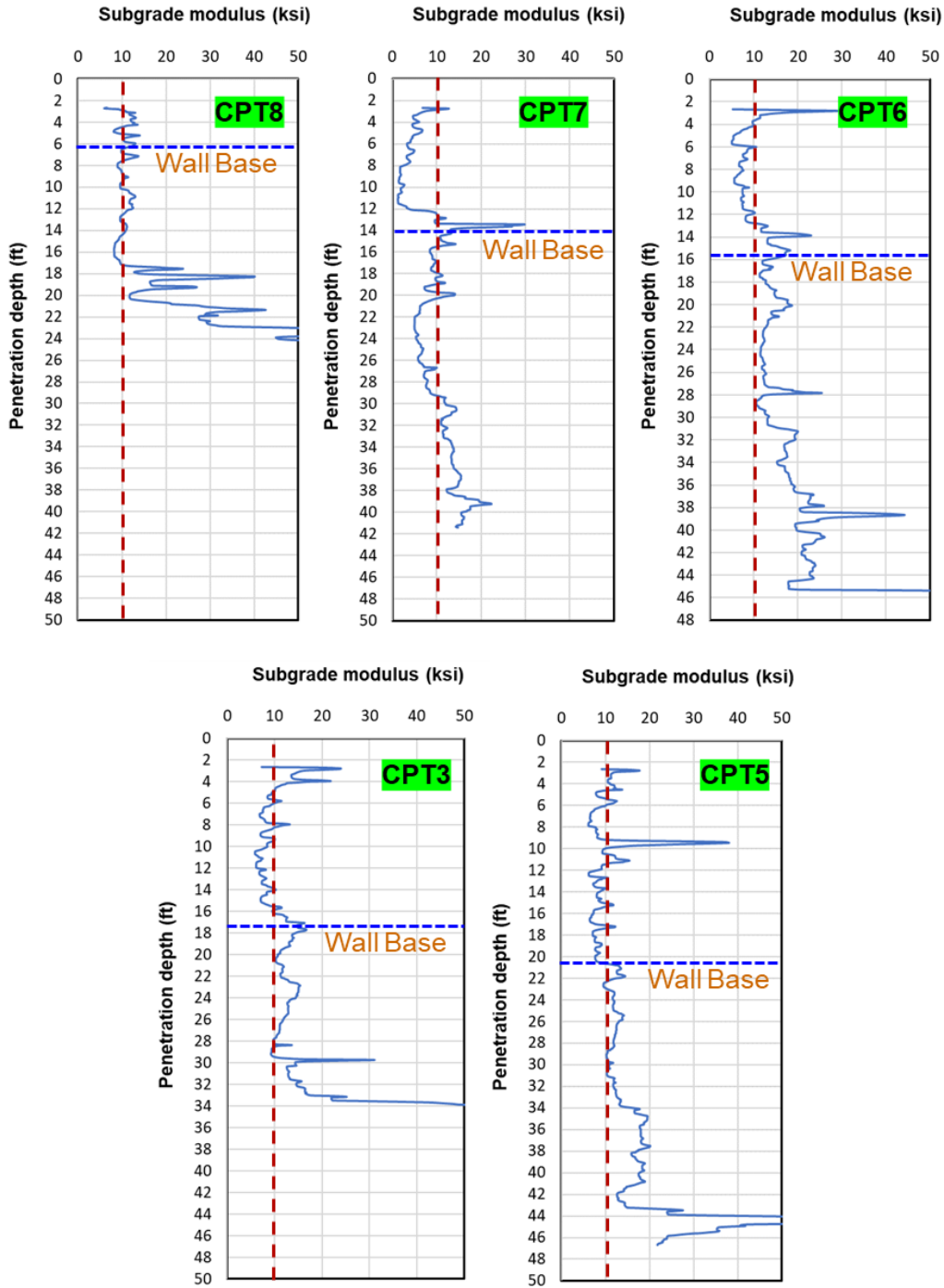


**Figure 35** Moduli of backfill materials and founding soils determined from CPT.

The height of the embankment decreases from east (i.e., bridge side) to west (i.e., exit side to Sabo Rd). In Figure 35, the bottom of the embankment is indicated at each CPT location. Except for CPT8 (Control section), soil moduli are overall less than 10 ksi for the entire embankment height at each CPT location. Below the embankment height, soil moduli of the founding soil are generally greater than 10 ksi but still less than 10 ksi at Location 7 up to about 29 ft below the pavement surface, which is 15 ft below the bottom of the embankment.

## C. Backfill/Subgrade Soil Characterization from Laboratory Tests

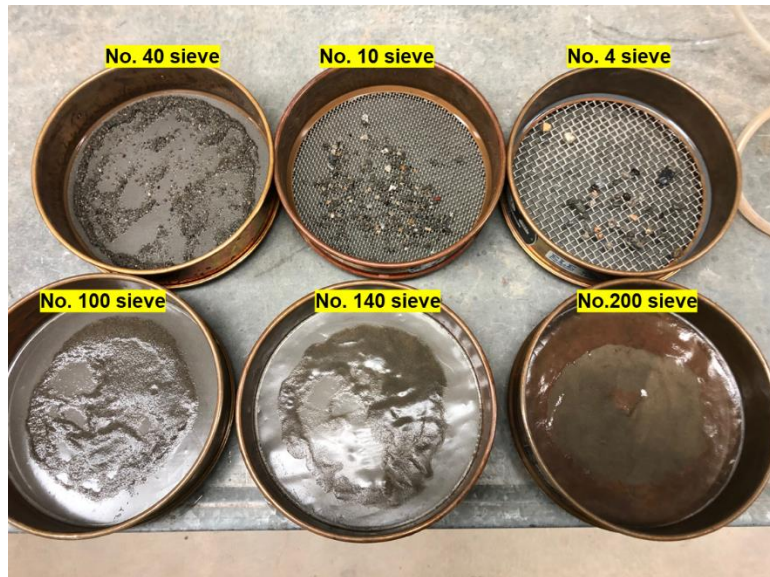
Soil samples were taken through the cored hole using a hand auger at Location 2 from depths of 20" to 38" below the pavement surface. A small amount of soil sample was also taken at Location 5 from depths of about 20" to 31" from the soils discharged by a drill auger bit of the CPT rig. Properties of soil samples taken from the test section were evaluated in the laboratory. The soil properties evaluated were:

- Particle Size Distributions
- Atterberg Limits
- Specific Gravity
- Water content
- Soil classification per USCS
- Soil classification per AASHTO

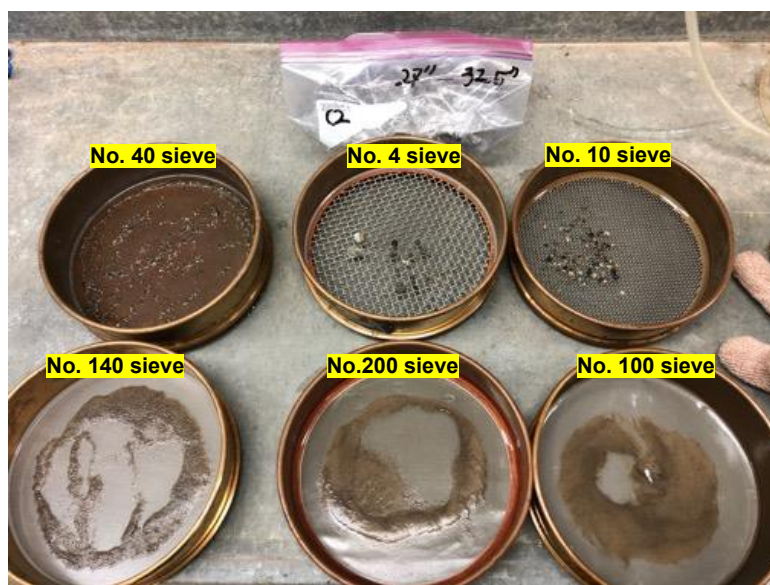
The following test procedures were followed:

- ASTM D1140-17: Standard Test Methods for Determining the Amount of Material Finer than 75- $\mu\text{m}$  (No. 200) Sieve in Soils by Washing
- ASTM D6913/D6913M-17: Standard Test Methods for Particle-Size Distribution (Gradation) of Soils Using Sieve Analysis
- ASTM D7928-21: Standard Test Method for Particle-Size Distribution (Gradation) of Fine-Grained Soils Using the Sedimentation (Hydrometer) Analysis
- ASTM D4318-17: Standard Test Methods for Liquid Limit, Plastic Limit, and Plasticity Index of Soils
- ASTM D854-14: Standard Test Methods for Specific Gravity of Soil Solids by Water Pycnometer
- ASTM D2216-19: Standard Test Methods for Laboratory Determination of Water (Moisture) Content of Soil and Rock by Mass
- ASTM D2487-17: Standard Practice for Classification of Soils for Engineering Purposes (Unified Soil Classification System)
- AASHTO M 145: Standard Specification for Classification of Soils and Soil–Aggregate Mixtures for Highway Construction Purposes

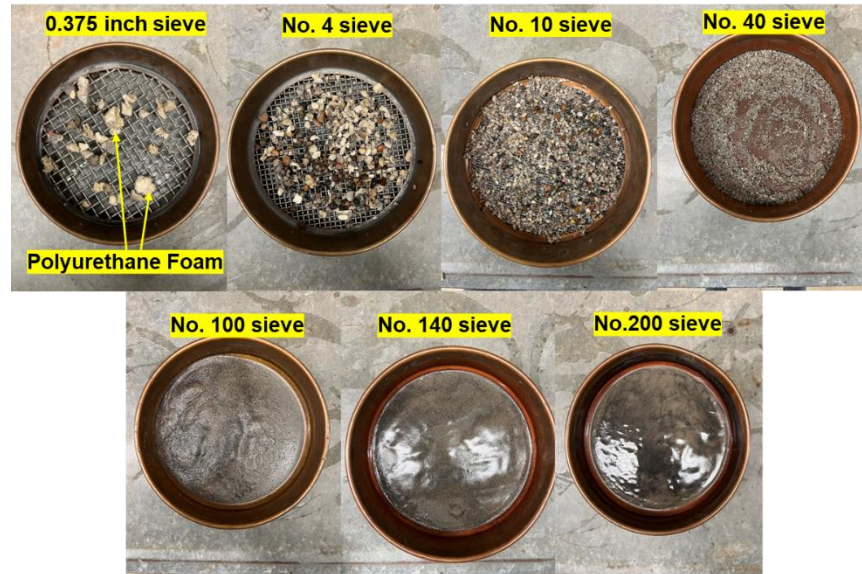
Particle size distributions were determined by wet sieving to determine percentage of fines more accurately. For soils passed through No. 200 sieve, a hydrometer test was performed. Photos of soil samples retained on each sieve and the hydrometer test setup are shown in [Figure 36](#). Note that pieces of polyurethane foam were observed from the CPT5 sample. Particle size distributions curves for all soil samples obtained from the wet sieve analysis and hydrometer analysis are presented in [Figure 37](#).



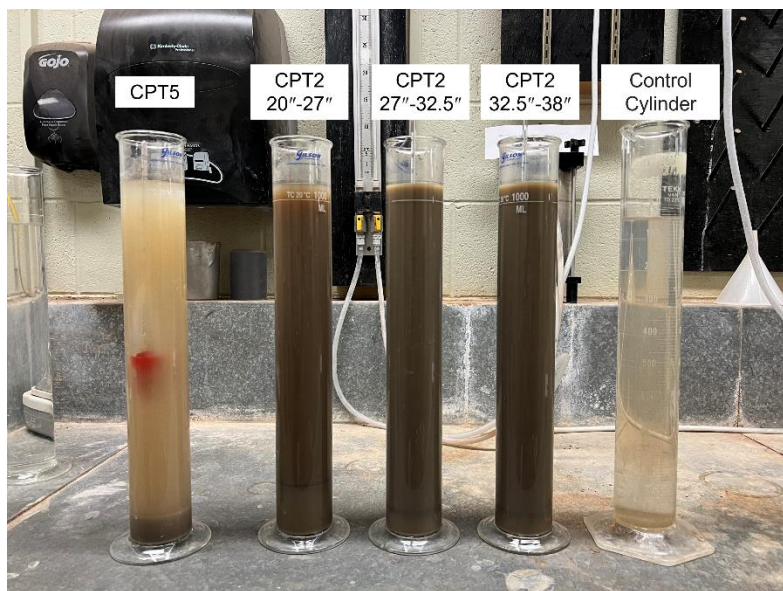
(a)



(b)



(c)



(d)

**Figure 36** Photos showing (a) soils retained on each sieve during wet sieving for CPT2 sample from 20" to 27", (b) CPT2 sample from 27" to 32.5 ", (c) CPT5 sample from 20" to 30", and (d) hydrometer testing in progress.

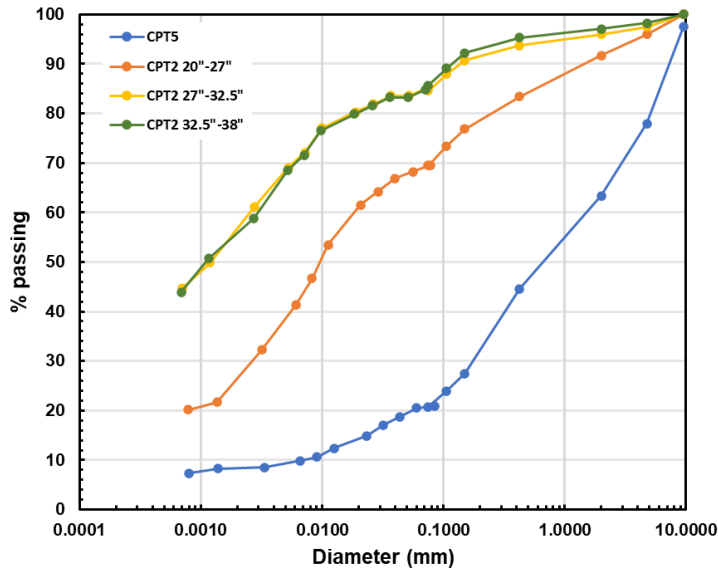


**Figure 37** Particle size distributions curves of all soil samples

Table 2 summarizes results from the laboratory tests conducted on the soil samples. The soil sample collected at Location 2 was classified as CH per USCS and A-7-6 per AASHTO, with PI values ranging between 43 and 48. On the other hand, the soil sample collected from the drill auger bit at Location 5 was classified SM or SC (Atterberg limit tests were not able to be conducted due to insufficient amount of soil that passed through No. 40) per USCS and A-2 per AASHTO. Natural moisture contents were about 35 percent for the clay sample (Location 2) and 21 percent for the sand sample (Location 5).

**Table 3** Summary of laboratory test results

Sample No.	Depth (in)	Soil Classification		Water content (%)	% passing #200	LL	PL	PI	LI	$G_s$
		USCS	AASHTO							
CPT2	20 – 27	CH	A-7-6	35	70	68	25	43	0.24	2.69
	27 - 32.5	CH	A-7-6	36	85	74	27	47	0.19	2.70
	32.5 - 38	CH	A-7-6	35	86	74	26	48	0.20	2.70
CPT5	20 - 30	SM or SC*	A – 2	23	21	-	-	-	-	-

Note: For the sample CPT5, the amount of the sample was not enough to conduct the Atterberg limit test.

### **III. Summary and Preliminary Recommendations**

Throughout the field investigation, potential issues have been identified in relation to a bridge abutment, MSE wall, and pavement. Specifically, it has been observed that there is a possibility of abutment movement on the Westbound side of the pavement. In addition, the lateral movement and wall tilting of the MSE wall appears to be having significant problems. With regards to the condition of the pavement, the inside lane does not exhibit any settlement and appears to have good sublayer support. However, the middle and outside lanes are having substantial settlement and deteriorated support. Furthermore, the joint separation between lanes is progressing considerably.

Several factors can be hypothesized to be causing these distresses, as mentioned above, such as the settlement and tilting of MSE walls, loss of embankment materials and wash-out, as well as potentially the collapse of drainage pipes. This results in joint separation and pavement settlement. Further field investigation specific to aforementioned factor is necessary for confirmation.

As a short-term strategy, a temporary repair may include filling the separated joints with flowable grout, which should minimize the infiltration of water through the joints. Long-term strategy should include addressing MSE wall issues, along with full-depth repairs and, if needed, hot mix asphalt overlays. In the case of the MSE wall, a geotechnical survey will be necessary to determine the most appropriate course of action.

### **References**

- Fowler W, D., Whitney P, D., Won, M., & Ha, S. (2012). *Pavement Repair Guidelines for Longitudinal Joints*. 7(November), 66p. [http://www.utexas.edu/research/ctr/pdf\\_reports/5\\_5444\\_01\\_1.pdf](http://www.utexas.edu/research/ctr/pdf_reports/5_5444_01_1.pdf)